Journal of Power Sources 223 (2013) 175–182

Contents lists available at SciVerse ScienceDirect

Journal of Power Sources

journal homepage: www.elsevier.com/locate/jpowsour

Conductivity, viscosity and density of $MClO_4$ (M = Li and Na) dissolved in propylene carbonate and γ-butyrolactone at high concentrations

K. Kuratani [a], N. Uemura [a,b], H. Senoh [a], H.T. Takeshita [b], T. Kiyobayashi [a,*]

[a] Research Institute for Ubiquitous Energy Devices, National Institute of Advanced Industrial Science and Technology (AIST), 1-8-31 Midorigaoka, Ikeda, Osaka 563-8577, Japan
[b] Department of Chemistry and Materials Engineering, Faculty of Chemistry, Materials and Bioengineering, Kansai University, 3-3-35 Yamate-cho, Suita, Osaka 564-8680, Japan

HIGHLIGHTS

- Comparison between transport properties of Li- and Na-based non-aqueous electrolytes.
- Density, viscosity and conductivity of $LiClO_4$ and $NaClO_4$ in PC and γBL were measured.
- Na-based electrolytes have 10–20% higher conductivity than Li-based ones at 0.5–2 M.
- Conductivities were analyzed based on a theory derived from the pseudolattice model.

GRAPHICAL ABSTRACT

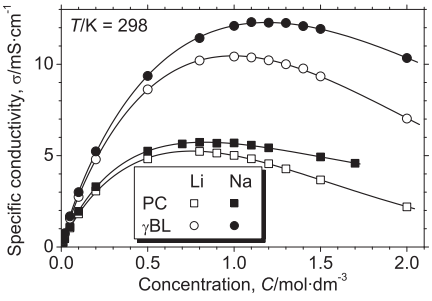

ARTICLE INFO

Article history:
Received 27 June 2012
Received in revised form
12 September 2012
Accepted 13 September 2012
Available online 23 September 2012

Keywords:
High concentration electrolyte
Nonaqueous
Cubic root law
Debye–Hückel–Onsager theory
Pseudolattice model

ABSTRACT

The solution density, viscosity and conductivity of $MClO_4$ (M = Li and Na) solutions in propylene carbonate and γ-butyrolactone are measured at the concentrations of <1.5–2.0 mol dm^{-3}. The partial volume of the solute, derived from the density, of $NaClO_4$ is greater than that of $LiClO_4$ as expected. $NaClO_4$ produces less viscous and more conductive solutions than $LiClO_4$ throughout the examined concentration range. Notably, the conductivity of the $NaClO_4$ solutions is 10–20% higher than that of the $LiClO_4$ solutions at $T/K = 298$. The validity of the empirical cubic root law, $\Lambda(C) = \Lambda_0 - AC^{1/3}$, is examined, where Λ and Λ_0 are the molar conductivities at the molarity C and at infinite dilution. The meaning of the slope A is interpreted in the theoretical framework of the pseudolattice model.

1. Introduction

Electrochemical devices based on nonaqueous lithium ion electrolytes are now ubiquitous in modern life from mobile phones to electric vehicles. The electrical conductivity and viscosity of the electrolyte solutions are a pair of fundamental transport phenomena that plays an important role in determining the performance of these electrochemical devices. Many nonaqueous solutions doped with Li salts have a maximum specific conductivity σ at around 1 mol dm^{-3}. The maximum in σ at a certain concentration can be qualitatively explained by the competition between the increase in the number of charge carriers and the dragging (negative) effect of interionic interactions. While a number of experimental data has been collected to cover these high concentrations [1–8], the theoretical understanding of the ionic transport in concentrated solutions is not yet fully established (see Section 3.3).

Meanwhile, attempts to replace Li with Na as a charge carrier in the electrochemical devices have been recently drawing attention

* Corresponding author. Tel.: +81 72 751 9651; fax: +81 72 751 9629.
E-mail address: kiyobayashi-t@aist.go.jp (T. Kiyobayashi).

0378-7753/$ – see front matter © 2012 Elsevier B.V. All rights reserved.
http://dx.doi.org/10.1016/j.jpowsour.2012.09.039

Table 1
Symbols in the present study.

Symbol	Quantity
C	Molarity (mol concentration)
C^*	Molarity at which σ is maximum
η	Viscosity of solution
η_0	Viscosity of pure solvent
η_r	Relative viscosity, η/η_0
Λ	Molar conductivity, σ/C
Λ_0	Λ at infinite dilution
Λ^*	σ_{max}/C^*
M_1	Molecular weight of solvent
M_2	Molecular weight of solute
n_1	Molar number of solvent
n_2	Molar number of solute
σ	Specific conductivity
σ_{max}	Maximum in σ
ρ	Density of solution
ρ_0	Density of pure solvent
$\overline{V_1^0}$	Molar volume of pure solvent
$\overline{V_2^0}$	Molar volume of pure solute (crystal)
$\overline{V_2}$	Partial molar volume of solute in solution

due to the possible scarcity and/or the geopolitical volatility of Li resources [9–17]. Based on the advent of Na ion devices in the future, one finds that fundamental data on Na-based electrolytes are lacking in the literature compared to the vast compilation of information about the Li-based ones.

In the present study, we focused our attention on the differences in the transport properties between Li- and Na-salts by choosing $LiClO_4$ and $NaClO_4$ dissolved in two nonaqueous solvents, propylene carbonate (PC) and γ-butyrolactone (γBL) as model systems. The conductivities and viscosities of the $LiClO_4$ and $NaClO_4$ solutions are compared on the basis of empirical formulas. In addition, the conductivity is analyzed in the framework of a theory derived from the pseudolattice model.

The symbols and basic properties of the solvents and solutes used in the present study are summarized in Tables 1 and 2.

2. Experimental

Preparation of the solutions and the setup of the cells for all the measurement were carried out in a dry-box in which the dew point of air was maintained below 210 K. Lithium perchlorate ($LiClO_4$, nominal purity 97%) and sodium perchlorate ($NaClO_4$, 96%) were purchased from Kanto Chemical. The solutes were used without further purification, as we confirmed that the solute recrystallized from tetrahydrofuran showed no significant difference in conductivity from the one without recrystallization. The purities were taken into account in weighing the solute. Solvents were purchased from Kishida Chemical; propylene carbonate (PC, purity > 99.5%, water content < 30 ppm) and γ-butyrolactone (γBL, purity > 99.5%, water content < 30 ppm). We first prepared the stock solutions of 2.0 mol dm^{-3} of $LiClO_4$-PC, $LiClO_4$-γBL and $NaClO_4$-γBL; and 1.7 mol dm^{-3} of $NaClO_4$-PC, in which the concentration of the latter one is limited by the solubility. The stock solutions were dried by using the type-5A molecular sieves for 72 h. The concentration of each electrolyte solution for the measurement was adjusted by diluting the stock solution with pure solvent. The water content of the solutions was maintained at less than 50 ppm, which was determined by the Karl Fischer titration method (831 KF Coulometer, Metrohm).

Table 2
Basic properties of the solvents and solutes.

Solvent	PC $CH_3(C_2H_3)O_2C{=}O$	γBL $(CH_2)_3OC{=}O$
Molecular weight, M_1/g mol^{-1}	102.1	86.1
Relative permittivity, ε_r	64.98	41.78
Dipole moment	4.94D	4.12D
Molar volume, $\overline{V_1^0}$/cm^3 mol^{-1}	85.1	76.6
Solute	$LiClO_4$	$NaClO_4$
Molecular weight, M_2/g mol^{-1}	106.4	122.4
Molar volume[a], $\overline{V_2^0}$/cm^3 mol^{-1}	43.8	49.2

[a] In crystalline state calculated from the crystallographic data.

The temperature of the solutions was controlled in a thermostat within $\Delta T/K = \pm 0.3$. The temperature of the thermostat was calibrated by a certified standard thermometer. The solutions were left in the thermostat for 30 min before the measurement to equilibrate the temperature. For all the measurements, three batches of solutions were prepared at each concentration. The results were presented as the mean of three runs using each solution batch.

The density of the solutions was measured by pycnometers with the nominal internal volume of 10 cm^3 of which the accurate value was calibrated by measuring the densities of degassed distilled water. The mass of the fluid was determined by subtracting the mass of the dried empty pycnometer from that of the filled one.

The viscosity was measured at $T/K = 278$, 288 and 298 by the rotating spindle method (Brookfield DV-II+) equipped with a UL attachment to cover the viscosity range of the present study. The viscometer was calibrated using standard reference oils (Nippon Grease, JS2.5, JS5 and JS50) covering the viscosity range from 1.9 to 42 mPa s at $T/K = 298$.

The conductivities of the solutions were measured at $T/K = 288$, 298 and 308. A beaker-type cell with four platinum electrodes was built in house [18]. The AC four-terminal method was adopted using an electrochemical analyzer (IviumStat). The applied current amplitude was 0.1 mA under which the amplitude of the voltage response ranged from *ca.* 1 to 1000 mV depending on the solution. The resistance was calculated from the I–V relation at 20 kHz at which the observed conductivity was confirmed to be independent of the frequency and free of noise. The resistance was converted to the specific conductivity σ by calibrating the cell with 0.01 and 0.1 mol dm^{-3} KCl aqueous solutions of which the specific conductivities are known to be 1.4085 and 12.853 mS cm^{-1}, respectively, at $T/K = 298$ [19].

3. Theoretical frameworks

3.1. Solution density and partial volume of the solute

The partial volume of the solute $\overline{V_2}$, *i.e.*, the increase in the solution volume when an infinitesimal amount of the solute is added to the solution at a given concentration, is defined by

$$\overline{V_2} \equiv \left(\frac{\partial V}{\partial n_2}\right)_{T,P,n_1} \tag{1}$$

where V is the volume of the solution, and n_1 and n_2 are the molar numbers of the solvent and solute, respectively. Note that $\overline{V_2}$ includes not only the volume of the solute molecule but also the change in the volume occupied by the solvent molecules that solvate the solute molecule. If the solution density is known as a function of the concentration $\rho = \rho(C)$, one can derive the partial molar volume as follows. The volume of the solution is related to the density as

$$V = \frac{n_1 M_1 + n_2 M_2}{\rho} \tag{2}$$

where M_1 and M_2 are the molecular weights of the solvent and solute. For all the systems examined in the present study, as shown

later in Section 4.1, the density ρ linearly varies with the molarity C as

$$\rho = \rho_0 + aC \tag{3}$$

$$= \rho_0 + a\frac{n_2}{V} \tag{4}$$

where ρ_0 is the density of the pure solvent and a is a constant. Introducing Eq. (4) into Eq. (2) and solving for V, one gets

$$\begin{aligned} V &= \frac{n_1 M_1 + n_2(M_2 - a)}{\rho_0} \\ &= n_1\overline{V_1^0} + n_2\frac{M_2 - a}{\rho_0} \end{aligned} \tag{5}$$

where $\overline{V_1^0}$ is the molar volume of the pure solvent. Hence, the partial molar volume of the solute Eq. (1) in this case is given by

$$\overline{V_2} = \frac{M_2 - a}{\rho_0}. \tag{6}$$

Namely, the linear dependency of the solution density on the molarity, Eq. (3), suggests the constant partial volume of the solute independent of the concentration.

3.2. Viscosity

The Jones–Dole empirical relation between the viscosity η and the molarity C is

$$\eta_r \equiv \frac{\eta}{\eta_0} = 1 + AC^{1/2} + BC + DC^2 \tag{7}$$

where η and η_0 are the viscosities of the solution and the pure solvent, respectively, and A, B and D are parameters [20]. The A- and B-terms can be physically interpretable [21–25]. On the other hand, although the interionic interactions seem to be related to it [26], the parameter D is currently considered empirical. The A-term is significant only at low concentrations, and thus often omitted at higher concentrations, *e.g.*, at C/mol dm^{-3} > 0.05. In such case,

$$\eta_r = 1 + BC + DC^n \tag{8}$$

where the square term in Eq. (7) is replaced by an n-th power term to deal with the general case in the discussion below. Hence,

$$\frac{\eta_r - 1}{C} = B + DC^{n-1}. \tag{9}$$

Namely, the plot $(\eta_r - 1)/C$ versus C^{n-1} should give a straight line of which the y-intercept and the slope give B and D, respectively. We will discuss the validities of these empirical equations in Section 4.2.

3.3. Conductivity

Classical theories of electrolyte conductivity are well documented in many textbooks such as Refs. [27,28]. In this section, only an outline that is pertinent to the present discussion is described.

3.3.1. Empirical cubic root ($C^{1/3}$) law of the molar conductivity

Suppose the molar conductivity Λ obeys the following formula

$$\Lambda = \Lambda_0 - AC^{1/n} \tag{10}$$

where Λ_0 is the molar conductivity at infinite dilution. In the vicinity of infinite dilution, Kohlrausch experimentally observed $n = 2$ to which the well-known Debye–Hückel–Onsager theory provides the theoretical basis (See Section 3.3.3). However, at higher concentrations, *e.g.*, 0.1 < C/mol dm^{-3} < 2 at which many electrochemical devices work, Eq. (10) with $n = 3$ is empirically known to better represent the experimental data. If $n = 3$ in Eq. (10),

$$\Lambda = \Lambda_0 - AC^{1/3}, \tag{11}$$

and the specific conductivity σ is given by

$$\sigma \equiv \Lambda C = C\left(\Lambda_0 - AC^{1/3}\right). \tag{12}$$

Solving $d\sigma/dC = 0$, one finds a maximum in Eq. (12) at

$$C^* = \left(\frac{3\Lambda_0}{4A}\right)^3. \tag{13}$$

The maximum in the specific conductivity σ_{max} at this molarity C^* is thus

$$\begin{aligned} \sigma_{max} &= C^*(\Lambda_0 - AC^{*1/3}) \\ &= C^*\frac{\Lambda_0}{4}. \end{aligned} \tag{14}$$

Eq. (14) suggests that, if the cubic root law Eq. (11) holds, the molar conductivity Λ^* at C^*, at which the specific conductivity shows the maximum σ_{max}, is one quarter of the molar conductivity at the infinite dilution regardless of the system; that is,

$$\begin{aligned} \Lambda^* &\equiv \frac{\sigma_{max}}{C^*} \\ &= \frac{\Lambda_0}{4}. \end{aligned} \tag{15}$$

When we normalize σ and C by σ_{max} and C^* as

$$y \equiv \frac{\sigma}{\sigma_{max}} \tag{16}$$

$$x \equiv \frac{C}{C^*}, \tag{17}$$

Eq. (12) is reduced to

$$y = 4x\left(1 - \frac{3}{4}x^{\frac{1}{3}}\right). \tag{18}$$

Notice that Eq. (18) no longer includes any adjustable parameters that depend on the system; *i.e.*, the law of corresponding state.

3.3.2. Walden's rule

Based on the continuum model, a rough relation between the molar conductivity Λ and the viscosity η is given by the Walden rule which is, for a singly charged species, derived from

$$\frac{k_B T}{6\pi\eta r} = D = \frac{k_B T}{eF}\lambda \tag{19}$$

where k_B is the Boltzmann constant; F the Faraday constant; e the unit charge; and D, r and λ are, respectively, the diffusion coefficient, the radius and the ionic conductivity of the drifting entity. This relation gives the Walden product as

$$\lambda\eta = \frac{eF}{6\pi}\frac{1}{r} \tag{20}$$

$$\propto \frac{1}{r}, \tag{21}$$

or in terms of the molar conductivity Λ,

$$\Lambda\eta \propto \frac{1}{r_+} + \frac{1}{r_-} \tag{22}$$

where r_+ and r_- are the radii of the cationic and anionic species. Because $\lim_{C\to 0}\eta = \eta_0$, *i.e.*, independent of the solute, one gets

$$\Lambda_0 \propto \frac{1}{r_+} + \frac{1}{r_-} \tag{23}$$

for a given solvent system.

3.3.3. Pseudolattice model

Since the advent of the Debye–Hückel–Onsager (DHO) theory, the model has undergone many modifications to extend its applicable range of concentrations. Several other approaches outside of the DHO theory have also been formulated, such as the mean spherical approximation, hyper-netted chain model, etc. (See, for example Ref. [28]). These theories, however, have not yet succeeded in satisfactorily explaining the general behavior of the conductivity at the molarity around C/mol dm^{-3} ~ 1.0 or higher. The Casteel–Amis formula, an entirely empirical equation of which the fitting parameters have no physical meaning, is widely used to precisely represent the experimental data at high concentrations [29]. Recently, a phenomenological treatment in the framework of the dissipation-feedback scheme [30], or theories based on the pseudolattice model [31–33] have been successfully applied to the conductivity of the highly concentrated electrolytes or, in some cases, of ionic liquids. (See these references and those cited therein for more details as well as the recent development of other theories.)

In the present study, for the sake of a straightforward comparison between the Li- and Na-salts, we adopted the formalism applied by Chagnes et al. [31,32]. The pseudolattice model has emerged through the observation that certain properties of concentrated ionic solutions can be well explained by assuming that the solution is composed of a hypothetical lattice-like structure [34,35]. A modification of the DHO theory by the pseudolattice model was proposed as follows: In the DHO theory, the molar conductivity Λ is expressed as

$$\Lambda = \Lambda_0 - (A_1 + A_2\Lambda_0)\kappa \tag{24}$$

where κ^{-1} is the mean radius of the ionic cloud around the central ion under consideration. A_1 and A_2 are respectively related to the electrophoresis and relaxation of the ionic cloud through the drift of the central ion. For the 1:1-electrolyte,

$$A_1 = \frac{N_A e^2}{3\pi\eta} \tag{25}$$

$$A_2 = \frac{1}{2+\sqrt{2}} \cdot \frac{e^2}{12\pi\varepsilon_0\varepsilon_r k_B T} \tag{26}$$

where N_A is Avogadro's number; ε_0 and ε_r are the permittivity of a vacuum and the relative permittivity.[1] The DHO theory suggests

$$\begin{aligned}\kappa &= \left(\frac{N}{V}\cdot\frac{e^2}{\varepsilon_0\varepsilon_r N_A k_B T}\right)^{\frac{1}{2}} \\ &= \left(\frac{2e^2 C}{\varepsilon_0\varepsilon_r k_B T}\right)^{\frac{1}{2}} \\ &\propto C^{\frac{1}{2}}.\end{aligned} \tag{27}$$

However, at high concentrations like C/mol dm^{-3} ~ 1, the radius of the ionic cloud κ^{-1}/nm ~ 0.3 which is of the same order of magnitude as the size of the ion itself, suggesting that the premises lying behind the DHO theory are no longer valid, nor are the terms derived from the theory, A_1 or A_2.

The idea of salvaging the DHO theory by the pseudolattice model at high concentrations is to replace the reciprocal radius of the ionic cloud κ, Eq. (27), by the following one [38]. The lattice energy per ion, E_L, for a 1:1-valent ionic crystal is

$$E_L = \alpha\frac{e^2}{r_0} \tag{28}$$

where α is the Madelung constant and r_0 is the nearest neighbor distance in the lattice. In the pseudolattice model of the electrolyte solution, the ions in the electrolyte solution are assumed to constitute a loose lattice-like structure of which the nearest neighbor distance is equal to the mean distance between cation and anion; *i.e.*,

$$r_0 = \left(\frac{V}{N}\right)^{\frac{1}{3}} \tag{29}$$

where V is the volume of the system and N is the total number of cations and anions. The model identifies the radius of the ionic cloud κ^{-1} to be the one that gives the same lattice energy, Eq. (28), when this countercharged ionic cloud interacts with the central ion; *i.e.*,

$$E_L = \frac{e^2}{\kappa^{-1}}. \tag{30}$$

Eqs. (28)–(30) yield

$$\begin{aligned}\kappa &= \frac{\alpha}{r_0} \\ &= \alpha\left(\frac{N}{V}\right)^{\frac{1}{3}}. \\ &= \alpha(2N_A C)^{\frac{1}{3}}\end{aligned} \tag{31}$$

where the factor "2" appears because n moles of a 1:1-electrolyte contain a total of $2n$ moles of ions. Notice that if C is expressed in the unit of "mol dm^{-3}" instead of "mol m^{-3}", C in Eq. (31) must be multiplied by 10^3 to conform to the MKSA system.

If we substitute Eq. (31) for κ in Eq. (24), the expression of the molar conductivity Λ based on the pseudolattice model is given by

$$\Lambda = \Lambda_0 - \alpha(B_1 + B_2\Lambda_0)C^{\frac{1}{3}} \tag{32}$$

where

$$B_1 = \frac{2^{\frac{1}{3}}}{3\pi}N_A^{\frac{4}{3}}e^2\cdot\frac{1}{\eta} \tag{33}$$

$$B_2 = \frac{2^{\frac{1}{3}}}{12\pi\left(2+\sqrt{2}\right)}\frac{N_A^{\frac{1}{3}}e^2}{\varepsilon_0 k_B}\cdot\frac{1}{\varepsilon_r T}. \tag{34}$$

[1] The denominator in A_2 may look different by the factor $4\pi\varepsilon_0$ from some references because of the conversion of the dated electromagnetic unit system into the current MKSA system. For instance, D in Refs. [36,37] and ε in Refs. [27,28] should read $4\pi\varepsilon_0\varepsilon_r$ in the present case.

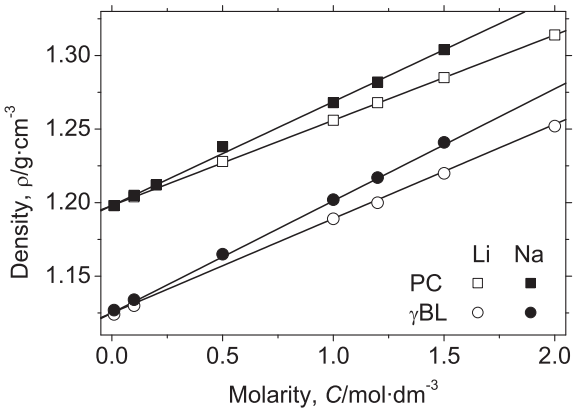

Fig. 1. Solution density ρ at $T/K = 298$.

Introducing the numerical values of the physical constants and taking care of the compatibility of the units, one gets the expression with the explicit units as

$$\frac{\Lambda}{\mathrm{S\,cm^2\,mol^{-1}}} = \frac{\Lambda_0}{\mathrm{S\,cm^2\,mol^{-1}}} - \alpha\left(\frac{17.451}{\eta/\mathrm{mPa\,s}} + \frac{1735.8}{\varepsilon_r(T/K)}\cdot\frac{\Lambda_0}{\mathrm{S\,cm^2\,mol^{-1}}}\right)\cdot\left(\frac{C}{\mathrm{mol\,dm^{-3}}}\right)^{\frac{1}{2}}. \quad (35)$$

4. Result and discussion

Numerical data at $T/K = 298$ presented in the present study as well as those at the other temperatures are available in the Supplementary material.

4.1. Density and partial volume of the solute

Fig. 1 plots the molarity dependence of the solution density $\rho = \rho(C)$ at $T/K = 298$. Throughout the measured concentration range, the densities are well represented by straight lines as in Eq. (3), or by explicitly introducing the units,

$$\frac{\rho}{\mathrm{g\,cm^{-3}}} = \frac{\rho_0}{\mathrm{g\,cm^{-3}}} + 10^{-3}\cdot\frac{a}{\mathrm{g\,mol^{-1}}}\cdot\frac{C}{\mathrm{mol\,dm^{-3}}}. \quad (36)$$

The result of the numerical optimization to Eq. (36) is summarized in Table 3. Also listed in the table is the partial molar volume of the solute $\overline{V_2}$ calculated by Eq. (6). One can find two features in the partial volume:

(i) $NaClO_4$ occupies *ca.* 3 cm^3 mol^{-1} more volume than $LiClO_4$ regardless of the solvent, *i.e.*,

$$\overline{V_2}(\mathrm{NaClO_4}) - \overline{V_2}(\mathrm{LiClO_4}) \sim 3\ \mathrm{cm^3\ mol^{-1}}$$

for each solvent.

(ii) Either solute occupies 2–3 cm^3 $mol^{-1}$of more volume in PC than in γBL, *i.e.*,

Table 3
Linear relation Eq. (36) between the density ρ and the molarity C, and the partial molar volume of the solute $\overline{V}_2$ at T/K = 298.

	PC		γBL	
	$LiClO_4$	$NaClO_4$	$LiClO_4$	$NaClO_4$
ρ_0/g cm^{-3}	1.198		1.125	
a/g mol^{-1}	58.0	70.6	64.1	76.2
$\overline{V}_2$/cm^3mol^{-1}	40.4	43.2	37.6	41.1

$$\overline{V_2}(\text{in PC}) - \overline{V_2}(\text{in } \gamma\mathrm{BL}) \sim 2 - 3\ \mathrm{cm^3\ mol^{-1}}$$

for each solute.

The larger ionic radius of Na^+ than Li^+, and accordingly the larger size in the "static" solvation shell of the Na-salt must be reflected in (i). Item (ii) suggests that γBL more densely solvates the solute than PC, whichever solute is solvated by them. The simpler molecular structure of γBL than PC may ease conforming to the solvation shell.

The ionic conductivity of Na^+ at infinite dilution, λ_0 (Na^+), is higher than that of Li^+, λ_0 (Li^+) [39]. As Eq. (23) suggests, the radius of the drifting cationic agency, r_+, is considered larger for Li^+ than for Na^+ because the former more strongly attracts the solvent than the latter. The present result confirms that the order of the static volume observed in $\overline{V_2}$ is contrary to the dynamic volume reflected in $1/\lambda_0$.

4.2. Viscosity

The viscosity η as a function of the molarity C at $T/K = 298$ is shown in Fig. 2(a). Either in PC or in γBL, $LiClO_4$ produces a more viscous solution than $NaClO_4$ at a given concentration. The difference between the $LiClO_4$- and $NaClO_4$-solutions expands at higher concentrations. In γBL, for example, while the $LiClO_4$ solution is about 10% more viscous than the $NaClO_4$ solution at C/mol dm^{-3} = 1.0, the difference is more than 30% at C/mol dm^{-3} = 2.0. In PC, the case is more prominent in that the gap is 20% at C/mol dm^{-3} = 1.0, which increases to 45% at C/mol dm^{-3} = 1.5.

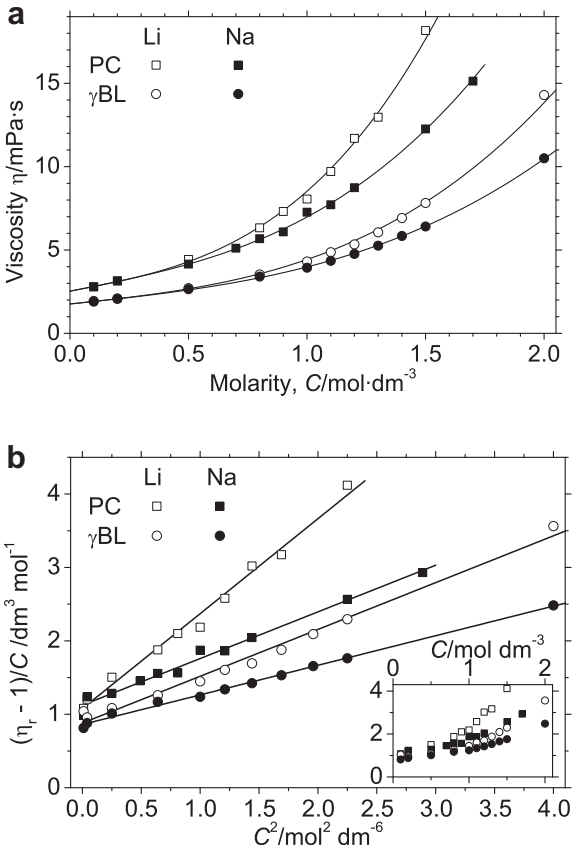

Fig. 2. (a) Viscosity η as a function of the molarity C at $T/K = 298$. (b) $(\eta_r-1)/C$ *vs.* C^2 (the inset is *vs.* C). Solid lines indicate the function optimized to Eq. (37).

Table 4
Viscosity of pure solvent η_0, and the optimized parameters B' and D' in Eq. (37) at $T/K = 298$.

	η_0 mPa s	$LiClO_4$		$NaClO_4$	
		B' dm^3 mol^{-1}	D' dm^9 mol^{-3}	B' dm^3 mol^{-1}	D' dm^9 mol^{-3}
PC	2.53	1.077	1.293	1.123	0.636
γBL	1.76	0.880	0.638	0.861	0.403

We found that the original Jones–Dole equation, *i.e.*, $n = 2$ in Eq. (8), does not well represent the experimental data at higher concentrations, such as at C/mol dm$^{-3} > 1.5$. By replacing the square term $n = 2$ with a cubic term $n = 3$, we obtained a better representation of the experimental data without increasing the number of fitting parameters as indicated by the solid lines in Fig. 2(a) and (b):

$$\eta_r = \frac{\eta}{\eta_0} = 1 + B'C + D'C^3 \tag{37}$$

or

$$\frac{\eta_r - 1}{C} = B' + D'C^2 \tag{38}$$

where we replaced the symbols B and D with B' and D' to distinguish from the original Jones–Dole equation Eq. (7). As shown in Fig. 2(b), the plot of $(\eta_r - 1)/C$ versus C^2 is closer to linear than that of versus C, which is obviously concave upward as in the inset figure. Table 4 summarizes the optimized parameters of B' and D' as well as the experimentally measured viscosities of the pure solvents η_0. Roughly speaking, in a given solvent, whereas the B'-parameters of $LiClO_4$ and $NaClO_4$ are close, D' of $LiClO_4$ is greater than that of $NaClO_4$, which is responsible for the increasing gap in the viscosity between these salts at higher concentrations. In the present study, we present these parameters purely from an empirical basis. Although the original D-parameter is considered empirical in the first place, the physical interpretation of the B-term, see for example Ref [25], does not hold any more for B'.

4.3. Conductivity

Fig. 3 plots the specific conductivity σ versus the molarity C at $T/K = 298$. Scales above the figure indicate the solvent to solute molar ratio n_1/n_2 for each solvent system.[2] The data are well represented by the empirical Casteel–Amis equation [29] as indicated by the solid line (See Supplementary material). The specific conductivity σ of the $LiClO_4$ solution in PC at 1.0 mol dm^{-3} and 298 K is in our study 5.01 mS cm^{-1}, which falls within the rather scattered values found in preceding studies; *i.e.*, 5.6 [1], 3.9 [41] and 4.356 mS cm^{-1} [42]. Our result of $\sigma(LiClO_4$in γBL, 1.0 mol dm^{-3}, 298 K)/mS cm^{-1} = 10.4 well coincides with the one determined by Chagnes et al., 10.9 mS cm^{-1} [31]. For the $NaClO_4$ solution in PC at 298 K, our result of 5.68 mS cm^{-1} at 0.9 mol dm^{-3} (=0.782 mol kg^{-1}) is comparable to 6.13 mS cm^{-1} which is reported as the conductivity of the same system at 0.78964 mol kg^{-1} [3].

The γBL solutions have higher conductivities than the PC solutions, for which the lower viscosity of γBL than PC is considered to some extent responsible. The conductivities of the $NaClO_4$ solutions are always higher than those of the corresponding $LiClO_4$ solutions. Especially, in the concentration range in which many electrochemical devices function ($0.5 < C$/mol dm$^{-3} < 1.5$), the conductivity of the $NaClO_4$ solution is 10–20% greater than that of the $LiClO_4$ solution. So long as the conductivity of the electrolyte is concerned, the sodium-based electrolyte solution can rival or surpass the lithium-based counterpart.

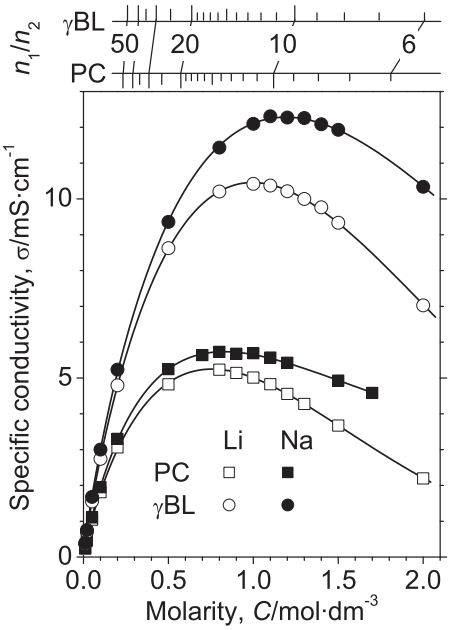

Fig. 3. Specific conductivity σ plotted *vs.* the molarity C of $LiClO_4$ and $NaClO_4$ dissolved in PC and γBL at $T/K = 298$. Solid lines are the result of the numerical optimization to the empirical Casteel–Amis function [29]. Scales above the figure indicate the solvent to solute molar ratio n_1/n_2 for each solvent system.

In γBL, the Walden product $\Lambda\eta$, Eq. (22), of the $NaClO_4$ solution is still greater than that of the $LiClO_4$ solution even at high concentrations, similar to the case of the dilute solutions. In PC, on the other hand, $\Lambda\eta$ of the $NaClO_4$ solution is not always higher than that of the $LiClO_4$ solution depending on the concentration. This suggests that the continuum model based on which the Walden rule is derived is no longer valid at high concentrations as pointed out by Brouillette et al. [8].

Table 5 summarizes the maximum in the specific conductivity σ_{max} at the molarity C^*, and the molar conductivity Λ^* at C^*, *i.e.*, $\Lambda^* \equiv \sigma_{max}/C^*$. Also listed in the table is the molar conductivity at infinite dilution divided by four, $\Lambda_0/4$, calculated from the data given in Refs. [39,40]. Eq. (15) holds fairly well for all the investigated systems, suggesting the empirical cubic root law, Eq. (11), well represents the solution conductivity at least in the vicinity of σ_{max}.

The validity of the cubic root law is also examined in Fig. 4 in which the molar conductivity Λ is plotted versus $C^{1/3}$. In γBL, the relation $\Lambda = \Lambda(C^{1/3})$ falls on a straight line in the range $0.45 < C^{1/3}$/mol$^{1/3}$ dm$^{-1} < 1.1$ or $0.1 < C$/mol dm$^{-3} < 1.3$. On the other hand, the linearity is fair, at best, for the PC systems. (This issue is revisited below in the discussion on the law of the corresponding state.) The results of the numerical optimization of the experimentally obtained Λ to Eq. (11) are listed in Table 6. The calculated molar conductivities at infinite dilution, Λ_0, well coincide with those reported in Ref. [39] for $LiClO_4$ and $NaClO_4$, and in Ref. [40] for $LiClO_4$. Either in PC or in γBL, the slope of the straight line in Λ *vs.* $C^{1/3}$ is more negative for $NaClO_4$ than for $LiClO_4$; *i.e.*,

$$\Lambda(NaClO_4) > \Lambda(LiClO_4). \tag{39}$$

Nonetheless, the conductivities of the $NaClO_4$ solutions exceed those of the $LiClO_4$ solutions because $\Lambda(NaClO_4)$ is not very high to

[2] Exactly speaking, n_1/n_2 depends on not only the solvent, but also the solute. However, the difference in n_1/n_2 between $LiClO_4$ and $NaClO_4$ is not recognizable in this scale.

Table 5
Maximum in the specific conductivity σ_{max} at the molarity C^* at $T/K = 298$. The molar conductivity Λ^* at this molarity C^* is compared with the molar conductivity at infinite dilution divided by four, $\Lambda_0/4$ (*cf.* Eq. (15)).

	PC		γBL	
	$LiClO_4$	$NaClO_4$	$LiClO_4$	$NaClO_4$
C^*/mol dm^{-3}	0.8	0.8	1.0	1.1
σ_{max}/mS cm^{-1}	5.23	5.73	10.4	12.3
Λ^*/S cm^2 mol^{-1}	6.54	7.16	10.4	11.2
$(\Lambda_0/4)^a$/S cm^2 mol^{-1}	6.69	6.97	9.80	10.0
$(\Lambda_0/4)^b$/S cm^2 mol^{-1}	6.84	–	10.6	–

[a] Calculated from Λ_0 in Refs. [39].
[b] Calculated from Λ_0 in Refs. [40].

cancel out, at higher concentrations, the higher molar conductivity at infinite dilution, $\Lambda_0(NaClO_4) > \Lambda_0(LiClO_4)$.

The difference in the slope A can be semi-quantitatively explained by the pseudolattice model. As Eq. (35) suggests, the higher Λ_0 leads to the higher A, if η and ε_r are assumed those of the solvent, not of the solution, though this assumption is arguable. In effect, Eq. (35) yields the slope A_{cal} in Table 6, if we hypothesize the Madelung constant of the pseudolattice to be of the regular fcc lattice, $\alpha = 1.748$ and Λ_0 to be the one that is obtained by the linear optimization in the present study. Regardless of the solute, $NaClO_4$ or $LiClO_4$, the calculated slope, A_{cal}, explains *ca.* 70% and 90% of the slope of the experimental data A_{exp} in PC and γBL, respectively, suggesting that the tendency, Eq. (39), is consistent with the model. To change the viewpoint, α_{cal} in Table 6 is obtained if we assume, conversely to the fcc lattice assumption, the Madelung constant α to be a fitting parameter to reproduce the experimental data. Whereas α_{cal} strongly depends on the solvent, it is not very

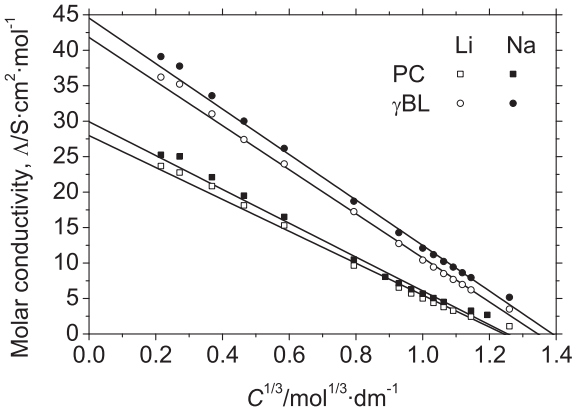

Fig. 4. Molar conductivity Λ *vs.* cubic root of molarity $C^{1/3}$.

Table 6
Result of the numerical optimization of Λ (at C/mol dm$^{-3} \geq 0.1$) to the cubic root law Eq. (11) at $T/K = 298$, compared with the parameters calculated based on the pseudolattice model.

	PC		γBL	
	$LiClO_4$	$NaClO_4$	$LiClO_4$	$NaClO_4$
Λ_0/S cm^2 mol^{-1}	28.0	29.9	41.8	44.5
$A_{exp}/10^2$ S cm^3 mol$^{-4/3}$	2.25	2.39	3.11	3.21
$A_{cal}/10^2$ S cm^3 mol$^{-4/3}$	1.64	1.67	2.75	2.82
A_{cal}/A_{exp}	0.731	0.702	0.886	0.879
α_{cal}	2.39	2.49	1.97	1.99

Λ_0, A_{exp}: Optimized parameters in Eq. (11) using experimental data; A_{cal}: Calculated slope in Eq. (35) under the assumption $\alpha = 1.748$ (fcc); α_{cal}: Calculated α in Eq. (35) in order to reproduce A_{exp}.

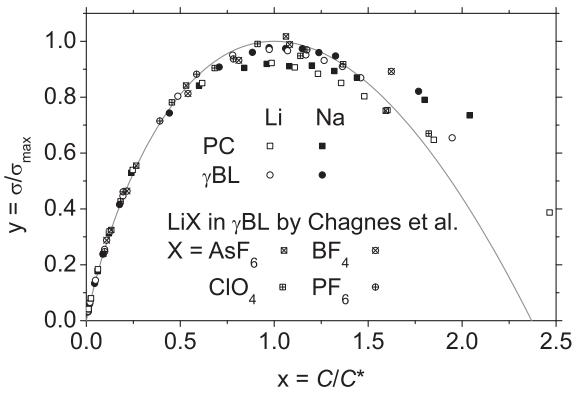

Fig. 5. Normalized conductivity $y \equiv \sigma/\sigma_{max}$ *vs.* normalized molarity $x \equiv C/C^*$. Chagnes et al.: Refs. [31,32] (See also Acknowledgement). Solid line indicates Eq. (18).

dependent on the solute. Using Raman spectroscopy, Chagnes et al. discussed that the higher slope of A_{exp} than A_{cal} for $LiClO_4$in γBL might be related to their observation that the degree of ion pairing, which reduces the fraction of charged species that contribute to the conductivity, was roughly constant over a wide concentration range [32]. Similarly, the formation of the ion pairs and the solvent-shared ion pairs, $Li^+\cdots solvent\cdots ClO_4^-$, is suggested in the concentrated solution of $LiClO_4$ [43,44]. The present study implies that the influence of the ion pairing on the slope, A, is more prominent in PC than in γBL, but the difference between $LiClO_4$ and $NaClO_4$ is less significant than the difference in the solvent.

Returning to the empirical cubic root law, Fig. 5 plots the normalized specific conductivity $y \equiv \sigma/\sigma_{max}$ versus the normalized molarity $x \equiv C/C^*$, in which σ_{max} and C^* were calculated from Λ_0 and A_{exp} in Table 6 using Eqs. (13) and (14). The result derived from the values obtained by Chagnes et al. [31,32] are also shown for the LiX solutions in γBL, in which σ_{max} and C^* were calculated in the same manner by the authors of the present article from their experimental data. In γBL at $x < 1.5$, the normalized conductivity y well follows the law of corresponding state, Eq. (18), for either solute. In PC, on the other hand, the deviation in the experimental data from Eq. (18) is appreciable even at $x \sim 1.0$. For either PC or γBL at $x > 1.5$, the normalized conductivity y is significantly underestimated from what is expected by the cubic root law, suggesting its applicable limit. As indicated by the n_1/n_2 scale in Fig. 3, the solvent to solute ratio becomes close to the number of the solvent molecules that solvate the solute molecule at these high concentrations. For example, the solvation number of Li^+ in $LiClO_4$ dissolved in ethylene carbonate is determined to be around four at C/mol dm$^{-3} < 1$ [45]. The mechanism that governs the transport phenomena seems to be modeled from the other viewpoint.

The present study provides only macroscopic data and their empirical treatment which must be complemented by microscopic studies such as Raman spectroscopy to elicit the molecular images of the Na^+ solvation as in the case of Li^+. We also hope that some theory can quantitatively bridge the gap between macroscopic properties and microscopic information for highly concentrated electrolyte solutions.

5. Conclusion

While the partial volume ($\overline{V_2}$) of the $NaClO_4$ solution is larger than that of the $LiClO_4$ solution, the fluidity ($1/\eta$) and the conductivity (σ or Λ) of the former are significantly higher than those of the latter throughout the concentration up to 1.5–2 mol dm^{-3}. Sodium-based solutions can serve as a good electrolyte for the

electrochemical devices as lithium-based ones at least with respect to the conductivity. The maxima in the specific conductivity (σ_{max}) roughly coincide with those expected from the empirical cubic root law, $\sigma_{max}/C^* = \Lambda_0/4$. The slope of the molar conductivity Λ *vs.* the cubic root of the molarity $C^{1/3}$ is semi-quantitatively interpretable in the framework of the pseudolattice model. Deviations from the cubic root law are more conspicuous in PC than in γBL.

Acknowledgment

We would like to express our sincere gratitude to Dr. A. Chagnes for having kindly provided us the numerical data of his experiment published in Refs. [31,32].

Appendix A. Supplementary material

Supplementary material related to this article can be found at http://dx.doi.org/10.1016/j.jpowsour.2012.09.039.

References

[1] J. Barthel, H.-J. Gores, G. Schmeer, Ber. Bunsenges. Phys. Chem. 83 (1979) 911–920.
[2] H.-J. Gores, J. Barthel, J. Solution Chem. 9 (1980) 939–954.
[3] J. Barthel, H.-J. Gores, P. Carlier, F. Feuerlein, M. Utz, Ber. Bunsenges. Phys. Chem. 87 (1983) 436–443.
[4] J. Barthel, Pure Appl. Chem. 57 (1985) 355–367.
[5] J. Barthel, H.-J. Gores, Pure Appl. Chem. 57 (1985) 1071–1082.
[6] A. Batkowska, G. Szymański, L. Werblan, J. Electroanal. Chem. 287 (1990) 229–238.
[7] J. Barthel, H.-J. Gores, Solution chemistry: a cutting edge in modern electrochemical technology, in: G. Mamantov, A.I. Popov (Eds.), Chemistry of Nonaqueous Solutions – Current Progress, VCH, New York, Weinheim and Cambridge, 1994 (Chapter 1).
[8] D. Brouillette, G. Perron, J.E. Desnoyers, Electrochim. Acta 44 (1999) 4721–4742.
[9] C. Delmas, J.J. Braconnier, C. Fouassier, P. Hagenmuller, Solid State Ionics 3–4 (1981) 165–169.
[10] J.J. Braconnier, C. Delmas, P. Hagenmuller, Mater. Res. Bull. 17 (1982) 993–1000.
[11] M. Dubois, D. Billaud, J. Solid State Chem. 127 (1996) 123–125.
[12] D.A. Stevens, J.R. Dahn, J. Electrochem. Soc. 147 (2000) 1271–1273.
[13] B.L. Ellis, W.R.M. Makahnouk, Y. Makimura, K. Toghill, L.F. Nazar, Nat. Mater. 6 (2007) 749–753.
[14] I.D. Gocheva, M. Nishijima, T. Doi, S. Okada, J. Yamaki, T. Nishida, J. Power Sources 187 (2009) 247–252.
[15] S. Komaba, C. Takei, T. Nakayama, A. Ogata, N. Yabuuchi, Electrochem. Commun. 12 (2010) 355–358.
[16] V. Palomares, P. Serras, I. Villaluenga, K.B. Hueso, J. Carretero-González, T. Rojo, Energy Environ. Sci. 5 (2012) 5884–5901.
[17] K. Kuratani, M. Yao, H. Senoh, N. Takeichi, T. Sakai, T. Kiyobayashi, Electrochim. Acta 76 (2012) 320–325.
[18] H. Senoh, T. Kiyobayashi, K. Tatsumi, N. Kuriyama, K. Tanimoto, J. Power Sources 164 (2007) 94–99.
[19] Y.C. Wu, K.W. Pratt, W.F. Koch, J. Solution Chem. 18 (1989) 515–528.
[20] G. Jones, M. Dole, J. Am. Chem. Soc. 51 (1928) 2950–2964.
[21] A. Einstein, Ann. Phys. 19 (1906) 289–306 (Correction in ibid. 34 (1911) 591-592).
[22] H. Falkenhagen, M. Dole, Phys. Z. 30 (1929) 611–622.
[23] D.J.P. Out, J.M. Los, J. Solution Chem. 9 (1980) 19–35.
[24] N.C. Dey, G. Kumar, B.K. Saikia, I. Haque, J. Solution Chem. 14 (1985) 49–58.
[25] H.D.B. Jenkins, Y. Marcus, Chem. Rev. 95 (1995) 2695–2724.
[26] M.M. Lencka, A. Anderko, S.J. Sanders, R.D. Young, Int. J. Thermophys. 19 (1998) 367–378.
[27] R.A. Robinson, R.H. Stokes, Electrolyte Solutions, second ed., Butterworths, London, 1959 (Chapter 7).
[28] J.O.'M. Bockris, A.K.N. Reddy, Modern Electrochemistry, vol. 1, Ionics, second ed.,, Plenum, New York and London, 1998 (Chapters 3 and 4).
[29] J.F. Casteel, E.S. Amis, J. Chem. Eng. Data 17 (1972) 55–59.
[30] H. Mercedes-Villullas, E.R. Gonzalez, J. Phys. Chem. B 109 (2005) 9166–9173.
[31] A. Chagnes, B. Carré, P. Willmann, D. Lemordant, Electrochim. Acta 46 (2001) 1783–1791.
[32] A. Chagnes, B. Carré, P. Willmann, D. Lemordant, J. Power Sources 109 (2002) 203–213.
[33] L.M. Varela, J. Carrete, M. García, L.J. Gallego, M. Turmine, E. Rilo, O. Cabeza, Fluid Phase Equilib. 298 (2010) 280–286.
[34] J.C. Ghosh, J. Chem. Soc. Trans. 113 (1918) 449–458.
[35] L.W. Bahe, J. Phys. Chem. 76 (1972) 1062–1071.
[36] L. Onsager, Phys. Z. 27 (1926) 388–392.
[37] L. Onsager, Phys. Z. 28 (1927) 277–298.
[38] G.W. Murphy, J. Chem. Soc. Faraday Trans. 2 79 (1983) 1607–1611.
[39] M. Salomon, E.J. Plichta, Electrochim. Acta 29 (1984) 731–735.
[40] M. Ue, J. Electrochem. Soc. 141 (1994) 3336–3342.
[41] B.K. Makarenko, E.A. Mendzheritskii, R.P. Sobolev, Yu.M. Povarov, P.A. Sereda, Sov. Electrochem. 10 (1974) 337–340.
[42] K.I. Tikhonov, V.A. Ivanova, B.A. Ravdel, J. Appl. Chem. USSR 50 (1977) 45–48.
[43] D. Battisti, G.A. Nazri, B. Klassen, R. Aroca, J. Phys. Chem. 97 (1993) 5826–5830.
[44] B. Klassen, R. Aroca, M. Nazri, G.A. Nazri, J. Phys. Chem. B 102 (1998) 4795–4801.
[45] S.A. Hyodo, K. Okabayashi, Electrochim. Acta 34 (1989) 1551–1556.